

Intermediate spin pair relaxation through modulation of isotropic hyperfine interaction in frequency-swept spin-dependent recombination in 4H-SiC F

Cite as: Appl. Phys. Lett. **120**, 062403 (2022); <https://doi.org/10.1063/5.0084378>

Submitted: 05 January 2022 • Accepted: 20 January 2022 • Published Online: 07 February 2022

 J. P. Ashton,  B. R. Manning,  S. J. Moxim, et al.

COLLECTIONS

F This paper was selected as Featured



[View Online](#)



[Export Citation](#)



[CrossMark](#)

 QBLOX



1 qubit

Shorten Setup Time

Auto-Calibration

More Qubits

Fully-integrated

Quantum Control Stacks

Ultrastable DC to 18.5 GHz

Synchronized <<1 ns

Ultralow noise



100s qubits

[visit our website >](#)

Intermediate spin pair relaxation through modulation of isotropic hyperfine interaction in frequency-swept spin-dependent recombination in 4H-SiC

Cite as: Appl. Phys. Lett. **120**, 062403 (2022); doi: [10.1063/5.0084378](https://doi.org/10.1063/5.0084378)

Submitted: 5 January 2022 · Accepted: 20 January 2022 ·

Published Online: 7 February 2022



View Online



Export Citation



CrossMark

J. P. Ashton,^{1,a)}  B. R. Manning,²  S. J. Moxim,³  F. V. Sharov,³  P. M. Lenahan,³  and J. T. Ryan¹ 

AFFILIATIONS

¹Alternative Computing Group, National Institute of Standards and Technology, Gaithersburg, Maryland 20899, USA

²High Frequency Technology Center, Santa Rosa, California 95403, USA

³Department of Engineering Science and Mechanics, The Pennsylvania State University, University Park, Pennsylvania 16802, USA

^{a)}Author to whom correspondence should be addressed: james.ashton@nist.gov

ABSTRACT

Electrically detected magnetic resonance (EDMR) measurements have been extended to sub-mT magnetic fields through utilization of frequency sweeping of the oscillating magnetic field, where conventional electron paramagnetic resonance-based measurements traditionally utilize magnetic field magnitude ramping. In spin-dependent transport measurements in devices, an oftentimes pervasive near-zero field magnetoresistance effect overwhelms the sub-mT regime. This magnetoresistance effect is independent of the RF drive. Thus, by utilizing a constant DC magnetic field and a frequency sweep of the RF magnetic field, the magnetoresistance effect is not detected, leaving only the EDMR response. Interesting EDMR-based phenomena emerge at sub-mT fields when the oscillating field magnitude approaches the static field, such as multiple-photon transitions caused by the emergence of Floquet spin states and Bloch–Siegert shifts. A spectral-narrowing effect also emerges as the static field is reduced. In this work, we show that the narrowing of the frequency-swept EDMR response with static field can be modeled by changes in intermediate spin-pair relaxation through modulation of hyperfine fields caused by stochastic perturbations from the environment. We utilize recently developed theory to model the relaxation of spin pairs and show that stochastic interactions of the electron spin with the environment yield both Floquet spin states and changes in intermediate spin-pair relaxation.

Published by AIP Publishing. <https://doi.org/10.1063/5.0084378>

Coupling to nuclear spins has pronounced effects on the lifetimes of defect electron spins at low magnetic fields. Nitrogen vacancy centers in diamond have defect electron spin lifetimes that are inversely proportional to the magnetic field. This phenomenon is caused by coupling of the electron spins to the ¹³C nuclear spin bath, which occurs when the magnetic field is on the order of the hyperfine coupling fields.¹ In pulsed electrically detected magnetic resonance (EDMR) of silicon (Si) doped with phosphorous, a similar increase in the spin lifetime with the decreasing magnetic field in the weak field regime has been reported and is due to a similar electron-nuclear hyperfine coupling effect.²

Furthermore, ultra-low field EDMR measurements have become ever more apparent in literature.^{3–10} In the ultra strong coupling regime, where the static and oscillating field magnitudes become comparable, exotic phenomena emerge from spins and spin pairs in

materials and devices, such as the spin-Dicke effect,¹⁰ multiple-photon transitions caused by Floquet spin states,^{11–13} organic magnetoresistance,^{14–16} and recently near-zero field magnetoresistance/zero field spin-dependent recombination (SDR).^{17–19}

Recently, a frequency-swept EDMR system was developed for sub-mT field measurements in 4H-SiC metal-oxide-semiconductor field-effect transistors (MOSFETs).²⁰ In this work, we utilized the 4H-SiC system to study spin pair relaxation within interface defects in 4H-SiC MOSFETs through studying the line shape of the frequency-swept (FS) EDMR response as a function of the static field.

This work can be well-understood by considering spin-dependent recombination (SDR) current, described in a seminal paper by Kaplan, Solomon, and Mott (KSM)²¹ and refined in later work.²² Consider the case when a device containing paramagnetic defects is subjected to a magnetic field B_0 and a microwave or RF field of energy

$E = h\nu$, h being Planck's constant and ν being the microwave or RF frequency. The magnetic field aligns the electron spin with or against the field. If both the conduction electron and unpaired electron spin have the same spin quantum number m_s in which m_s can either be $+1/2$ or $-1/2$, the transition of the conduction electron into the paramagnetic defect will be forbidden by the Pauli exclusion principle. However, resonance causes some defect electron spins to flip, enabling the capture of the conduction band electron because the conduction band electron now has the opposite spin of the defect electron. The captured electron is now available for electron-hole recombination. This process causes a change to the recombination current. Thus, the SDR response is caused by a conversion of intermediate triplet state spin pairs in which spin angular momentum is not conserved upon an SDR event, to intermediate singlet state spin pairs, in which spin angular momentum is conserved upon an SDR event. It should be noted that the sensitivity of the SDR response is nearly magnetic field- and frequency-independent, enabling detection of SDR at ultra-low magnetic fields.

The SDR resonance conditions depend on the defects' local environment. In relatively simple cases, the effect of the defect environment can be described via a spin Hamiltonian of the form,^{23–26}

$$\mathcal{H} = \mu_B \hat{\mathbf{B}}^T \cdot \mathbf{g} \cdot \hat{\mathbf{S}} + \sum_i \hat{\mathbf{I}}_i^T \cdot \mathbf{A}_i \cdot \hat{\mathbf{S}}. \quad (1)$$

Here, $\hat{\mathbf{B}}$ is the applied magnetic field vector ($\hat{\mathbf{B}} = B_0 \hat{k}$), \mathbf{g} is a second rank tensor whose parameters depend on the spin-orbit coupling interactions, $\hat{\mathbf{S}}$ is the electron spin angular momentum operator, $\hat{\mathbf{I}}_i$ is the nuclear spin angular momentum operator for the i th nucleus, and \mathbf{A}_i is the hyperfine coupling tensor for the i th nucleus. Resonance occurs when the RF or microwave energy matches the energy of the electron spins via (1). (This analysis does not fully describe all aspects of the defects under study, but it is sufficient for the purposes of this Letter.)

The linewidth of the observed unsaturated resonance response will depend on several physical phenomena, such as the spin relaxation times associated with the paramagnetic defects, broadening due to nearby hyperfine peaks within the central response, and the distribution of g-tensor components in the material system.²⁷ At ultra-low frequencies, the effects of hyperfine broadening will typically not be observed because most hyperfine field-splitting occurs at significantly greater fields than the response. Additionally, while frequency variation will cause a slight variation in the distribution due to lattice disorder, this effect scales linearly with frequency and is minimized at lower frequencies. Thus, only one main physical phenomena is left that accounts for the ultra-low frequency FS-EDMR linewidth: the spin relaxation times of the paramagnetic defects within the device system.

The ultra-low field FS-EDMR measurements were performed on a custom-built system. The experimental apparatus utilizes a custom-built 4" electromagnet with three sets of coils for greater field uniformity and built in modulation coils. The electromagnet is situated inside a three-layer cylindrical μ -metal zero-Gauss chamber with outer shield 2.8 m long and 0.6 m in diameter. We utilize a bipolar power supply for magnet power, a temperature-compensated Gaussmeter and Hall probe, a preamplifier, a virtual lock-in amplifier, a rf source fed into a custom-built resonator with diameter 6.6 mm with 9 turns, and a 1 GHz oscilloscope for power monitoring. Magnetic field

modulation is supplied from the computer, amplified by a stereo amplifier, and subsequently fed into the built-in modulation coils. The details of the spectrometer operation are reported elsewhere.²⁰

The samples utilized are n-channel 4H-SiC MOSFETs with a thermal oxide-nitride-oxide (ONO) oxide with thickness 50 nm and a gate area of $250 \times 20 \mu\text{m}^2$. We utilize the bipolar amplification effect (BAE) measurement.^{28,29} In BAE, the drain-to-body junction is forward biased well past the junction built-in voltage and the gate is biased close to, but below, inversion. The body is connected to ground. Subsequent SDR current is monitored through the source. This measurement is sensitive to defects with energy levels near the vicinity of the middle of the 4H-SiC bandgap. The uncertainties in our measurements of linewidth and B_1 are no greater than ± 0.2 MHz and ± 0.01 mT, respectively. All measurements were performed at room temperature.

In work by Fedin *et al.*,^{30,31} spin relaxation in weak magnetic fields is modeled within the framework of Redfield theory,³² showing that modulation of the isotropic (and anisotropic) hyperfine interaction causes an alteration in the relaxation rates of spin pairs coupled to nuclear spins. Their analysis^{30,31} shows that one may model the recombination rate R as a function of the electron Zeeman frequency ω_e as

$$R = \frac{(C_1^2 - C_2^2)^2}{2} \frac{\overline{\delta a^2} \tau_c}{1 + (\omega_e^2 + a^2) \tau_c^2}. \quad (2)$$

Here, C_1 and C_2 are functions of the hyperfine coupling a and the electron Zeeman frequency ω_e ^{30,31} and τ_c is the correlation time of the stochastic process described by a time dependent perturbation Hamiltonian, which in turn describes interactions with the electronic environment.³³ δa is defined as $a(t) - \bar{a}$, which is essentially the modulated hyperfine coupling. The coupling of the electron spin with a single $I = 1/2$ nucleus is illustrated in Fig. 1(a). Here, we represent the environment as oscillating fields to show how it acts to modulate the hyperfine coupling. One could imagine, for simplicity, that (2) could be derived by considering the energy levels from an electron interacting with a single spin $I = 1/2$ nucleus. If one were to consider the Breit-Rabi expressions for the electron energy levels,^{23,34} neglecting the nuclear Zeeman frequency, the spin-Hamiltonian of the stochastically modulated hyperfine interaction is $\mathcal{H}(t) = \delta a(t) \mathbf{I} \cdot \mathbf{S}$. Utilizing this stochastic perturbative Hamiltonian, the relaxation rate may then be calculated via Redfield theory.³² The energy level diagram for this system is shown in Fig. 1(b).

Figure 2 shows FS-EDMR data on the 4H-SiC MOSFET taken at five static magnetic fields, $B_0 = 0.1, 0.2, 0.3, 0.4,$ and 0.5 mT. Here, B_1 was 0.015 mT (calculated both through Faraday's law of induction and verified through measurements of the Bloch-Siegert shift).^{12,20} Note that with increasing B_0 , a broadening of the FS-EDMR response is observed. This broadening effect can be modeled well via (2). In Fig. 3, we plot the linewidth of the FS-EDMR response as a function of static field B_0 , with the linewidth data displayed on the left y-axis. On the right y-axis, we plot (2) normalized by $\overline{\delta a^2} \tau_c$. Note the fairly close correspondence between the curve shape of (2) and the linewidth data. In this fit, we utilize a coupling constant of 5.6 MHz, which corresponds to 0.2 mT. The 0.2 mT coupling constant agrees well with that extracted from near-zero field spin-dependent charge pumping (NZFSDCP) measurements in similar 4H-SiC MOSFET devices in a recent paper by Anders *et al.*³⁵ Since the shape of the fit of (2) matches

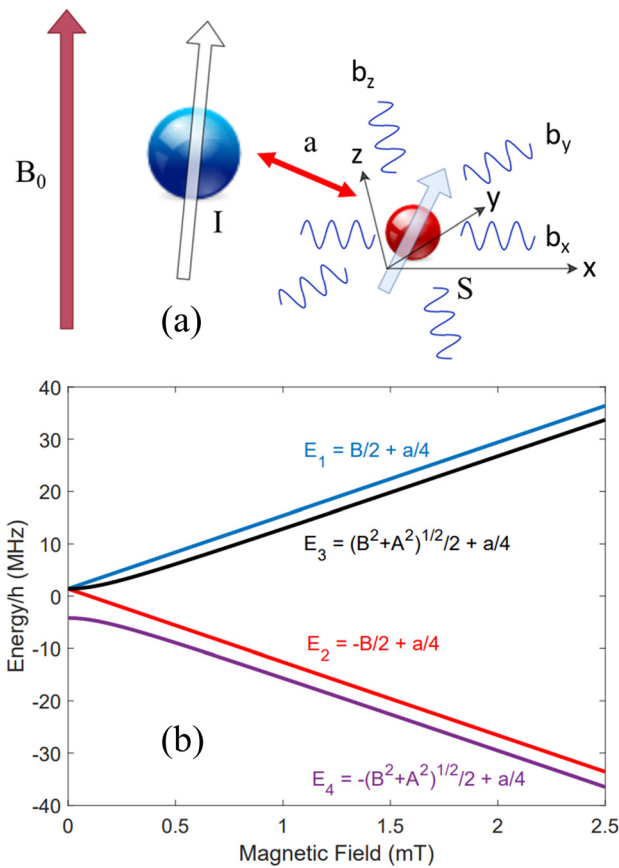


FIG. 1. (a) Illustration of an electron (red smaller sphere) coupled (with strength a) to a spin $I = 1/2$ nucleus (blue larger sphere) with the electron-nuclear interaction also coupled to a stochastic environment whose components are described by b_x , b_y , and b_z . (b) The Breit-Rabi^{24,34} energy solutions for the simplified case of an electron interacting with a single spin $I = 1/2$ nucleus. Here, a coupling constant of 5.6 MHz (0.2 mT) was utilized.³⁵

well with the linewidth data, we argue that we observe the same hyperfine interactions in this work.

While the experiment performed yields physics that is more complicated than that described by the simple model of isotropic hyperfine coupling modulation, one should note that the coupling of each defect spin to a magnetic nucleus will statistically vary from defect to defect. Thus, the utilization of an isotropic coupling assumes that there is an average hyperfine coupling over the ensemble of defect electron spins. This assumption simplifies the analysis and yields a relatively accurate qualitative understanding of the relaxation process. We are able to extract a coupling of 0.2 mT, which agrees well with recent work in models of 4H-SiC MOSFET NZFSDCP measurements.³⁵

This work also demonstrates that ultra-low field FS-EDMR can provide information about the effect of the environment and hyperfine interactions on spin relaxation. Future work will consist of utilizing temperature to further alter the spin relaxation times to yield a more quantitative analysis.

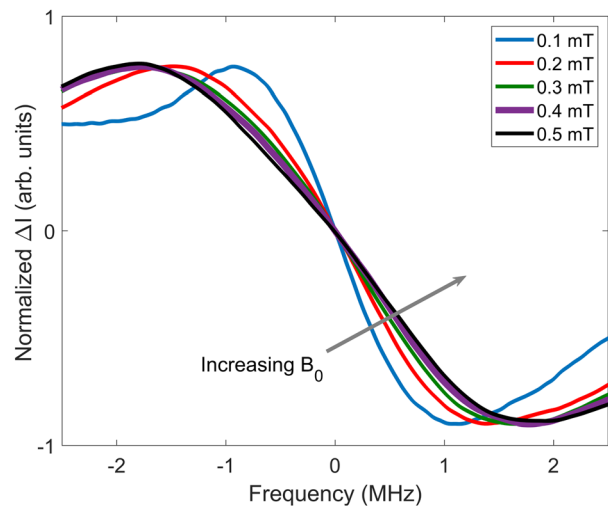


FIG. 2. FS-EDMR data taken at five static fields $B_0 = 0.1, 0.2, 0.3, 0.4,$ and 0.5 mT. The frequency axis has been offset to 0 for illustration of the broadening with B_0 . The amplitudes ΔI have been normalized.

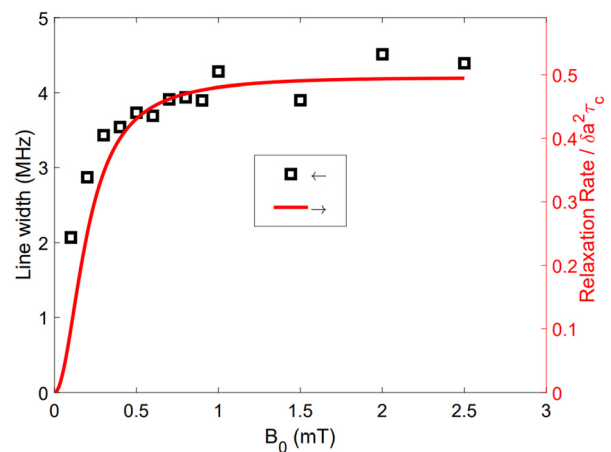


FIG. 3. (left axis) FS-EDMR linewidth as a function of B_0 . (right axis) Expression (2) normalized by $\delta a^2 \tau_c$. Here, an isotropic coupling constant a of 5.6 MHz was utilized. τ_c was set to 1 ns.

This work at Penn State was supported by the U.S. Army Research Laboratory. Any opinions, findings, conclusions, or other recommendations expressed herein are those of the authors and do not necessarily reflect the views of the U.S. Army Research Laboratory. This work was also supported by the Air Force Office of Scientific Research under Award No. FA9550-17-1-0242.

AUTHOR DECLARATIONS

Conflict of Interest

The authors have no conflicts to disclose.

DATA AVAILABILITY

The data that support the findings of this study are available from the corresponding author upon reasonable request.

REFERENCES

- ¹N. Zhao, S.-W. Ho, and R.-B. Liu, “Decoherence and dynamical decoupling control of nitrogen vacancy center electron spins in nuclear spin baths,” *Phys. Rev. B* **85**, 115303 (2012).
- ²L. Dreher, F. Hoehne, H. Morishita, H. Huebl, M. Stutzmann, K. M. Itoh, and M. S. Brandt, “Pulsed low-field electrically detected magnetic resonance,” *Phys. Rev. B* **91**, 075314 (2015).
- ³M. A. Anders, P. M. Lenahan, C. J. Cochrane, and J. Van Tol, “Physical nature of electrically detected magnetic resonance through spin dependent trap assisted tunneling in insulators,” *J. Appl. Phys.* **124**, 215105 (2018).
- ⁴G. Joshi, R. Miller, L. Ogden, M. Kavand, S. Jamali, K. Ambal, S. Venkatesh, D. Schurig, H. Malissa, J. M. Lupton, and C. Boehme, “Separating hyperfine from spin-orbit interactions in organic semiconductors by multi-octave magnetic resonance using coplanar waveguide microresonators,” *Appl. Phys. Lett.* **109**, 103303 (2016).
- ⁵H. Morishita, L. S. Vlasenko, H. Tanaka, K. Semba, K. Sawano, Y. Shiraki, M. Eto, and K. M. Itoh, “Electrical detection and magnetic-field control of spin states in phosphorus-doped silicon,” *Phys. Rev. B* **80**, 205206 (2009).
- ⁶M. Brandt, M. Bayerl, M. Stutzmann, and C. Graeff, “Electrically detected magnetic resonance of $a-si:h$ at low magnetic fields: The influence of hydrogen on the dangling bond resonance,” *J. Non-Cryst. Solids* **227–230**, 343–347 (1998).
- ⁷T. Grünbaum, S. Milster, H. Kraus, W. Ratzke, S. Kurrmann, V. Zeller, S. Bange, C. Boehme, and J. M. Lupton, “OLEDs as models for bird magnetoception: Detecting electron spin resonance in geomagnetic fields,” *Faraday Discuss.* **221**, 92–109 (2020).
- ⁸S. Milster, T. Grünbaum, S. Bange, S. Kurrmann, H. Kraus, D. M. Stoltzfus, A. E. Leung, T. A. Darwish, P. L. Burn, C. Boehme, and J. M. Lupton, “Perdeuterated conjugated polymers for ultralow-frequency magnetic resonance of OLEDs,” *Angew. Chem., Int. Ed.* **59**, 9388–9392 (2020).
- ⁹D. M. Stoltzfus, G. Joshi, H. Popli, S. Jamali, M. Kavand, S. Milster, T. Grünbaum, S. Bange, A. Nahlawi, M. Y. Teferi, S. I. Atwood, A. E. Leung, T. A. Darwish, H. Malissa, P. L. Burn, J. M. Lupton, and C. Boehme, “Perdeuteration of poly[2-methoxy-5-(2-ethylhexyloxy)-1,4-phenylenevinylene] (d-MEH-PPV): Control of microscopic charge-carrier spin-spin coupling and of magnetic-field effects in optoelectronic devices,” *J. Mater. Chem. C* **8**, 2764–2771 (2020).
- ¹⁰D. P. Waters, G. Joshi, M. Kavand, M. E. Limes, H. Malissa, P. L. Burn, J. M. Lupton, and C. Boehme, “The spin-Dicke effect in OLED magnetoresistance,” *Nat. Phys.* **11**, 910–914 (2015).
- ¹¹S. Jamali, V. V. Mkhitarian, H. Malissa, A. Nahlawi, H. Popli, T. Grünbaum, S. Bange, S. Milster, D. Stoltzfus, A. E. Leung, T. A. Darwish, P. L. Burn, J. M. Lupton, and C. Boehme, “Floquet spin states in OLEDs,” *Nat. Commun.* **12**, 465 (2021).
- ¹²J. P. Ashton and P. M. Lenahan, “Multiple-photon transitions in electrically detected magnetic resonance measurements of $4h$ -SiC transistors,” *Phys. Rev. B* **102**, 020101 (2020).
- ¹³H. Kraus, V. A. Soltamov, D. Riedel, S. Väh, F. Fuchs, A. Sperlich, P. G. Baranov, V. Dyakonov, and G. V. Astakhov, “Room-temperature quantum microwave emitters based on spin defects in silicon carbide,” *Nat. Phys.* **10**, 157–162 (2014).
- ¹⁴A. J. Schellekens, W. Wagemans, S. P. Kersten, P. A. Bobbert, and B. Koopmans, “Microscopic modeling of magnetic-field effects on charge transport in organic semiconductors,” *Phys. Rev. B* **84**, 075204 (2011).
- ¹⁵N. J. Harmon and M. E. Flatté, “Semiclassical theory of magnetoresistance in positionally disordered organic semiconductors,” *Phys. Rev. B* **85**, 075204 (2012).
- ¹⁶N. J. Harmon and M. E. Flatté, “Organic magnetoresistance from deep traps,” *J. Appl. Phys.* **116**, 043707 (2014).
- ¹⁷J. P. Ashton, S. J. Moxim, P. M. Lenahan, C. G. McKay, R. J. Waskiewicz, K. J. Myers, M. E. Flatte, N. J. Harmon, and C. D. Young, “A new analytical tool for the study of radiation effects in 3-D integrated circuits: Near-zero field magnetoresistance spectroscopy,” *IEEE Trans. Nucl. Sci.* **66**, 428–436 (2019).
- ¹⁸C. J. Cochrane and P. M. Lenahan, “Zero-field detection of spin dependent recombination with direct observation of electron nuclear hyperfine interactions in the absence of an oscillating electromagnetic field,” *J. Appl. Phys.* **112**, 123714 (2012).
- ¹⁹N. J. Harmon, S. R. McMillan, J. P. Ashton, P. M. Lenahan, and M. E. Flatte, “Modeling of near zero-field magnetoresistance and electrically detected magnetic resonance in irradiated Si/SiO₂ MOSFETs,” *IEEE Trans. Nucl. Sci.* **67**, 1669–1673 (2020).
- ²⁰J. P. Ashton, B. R. Manning, W. R. Barker, and P. M. Lenahan, “Ultra-low field frequency-swept electrically detected magnetic resonance,” *J. Appl. Phys.* **129**, 083903 (2021).
- ²¹D. Kaplan, I. Solomon, and N. Mott, “Explanation of the large spin-dependent recombination effect in semiconductors,” *J. Phys., Lett.* **39**, 51–54 (1978).
- ²²F. C. Rong, W. R. Buchwald, E. H. Poindexter, W. L. Warren, and D. J. Keeble, “Spin-dependent Shockley-read recombination of electrons and holes in indirect-band-gap semiconductor p-n junction diodes,” *Solid State Electron.* **34**, 835–841 (1991).
- ²³W. Gordy, *Theory and Applications of Electron Spin Resonance* (John Wiley & Sons, New York, 1980), p. 625.
- ²⁴C. Slichter, *Principles of Magnetic Resonance*, 3rd ed. (Springer-Verlag, Berlin/Heidelberg/New York/London/Paris/Tokyo/Hong Kong, 1978).
- ²⁵J. A. Weil, J. R. Bolton, and J. E. Wertz, *Electron Paramagnetic Resonance—Elementary Theory and Practical Applications* (Wiley, New York, 1994), p. 568.
- ²⁶D. Goldfarb and S. Stoll, *EPR Spectroscopy: Fundamentals and Methods* (John Wiley & Sons, 2018).
- ²⁷P. H. Rieger, *Electron Spin Resonance—Analysis and Interpretation* (Royal Society of Chemistry, 2007), pp. 96–97.
- ²⁸T. Aichinger and P. M. Lenahan, “Giant amplification of spin dependent recombination at heterojunctions through a gate controlled bipolar effect,” *Appl. Phys. Lett.* **101**, 083504 (2012).
- ²⁹J. P. Ashton, S. J. Moxim, A. D. Purcell, P. M. Lenahan, and J. T. Ryan, “A quantitative model for the bipolar amplification effect: A new method to determine semiconductor/oxide interface state densities,” *J. Appl. Phys.* **130**, 134501 (2021).
- ³⁰M. V. Fedin, P. A. Purtov, and E. G. Bagryanskaya, “Spin relaxation of radicals in low and zero magnetic field,” *J. Chem. Phys.* **118**, 192–201 (2003).
- ³¹M. Fedin, P. Purtov, and E. Bagryanskaya, “Anisotropic hyperfine interaction-induced spin relaxation in a low magnetic field,” *Chem. Phys. Lett.* **339**, 395–404 (2001).
- ³²A. G. Redfield, “On the theory of relaxation processes,” *IBM J. Res. Dev.* **1**, 19–31 (1957).
- ³³V. V. Mkhitarian, C. Boehme, J. M. Lupton, and M. E. Raikh, “Two-photon absorption in a two-level system enabled by noise,” *Phys. Rev. B* **100**, 214205 (2019).
- ³⁴G. Breit and I. I. Rabi, “Measurement of nuclear spin,” *Phys. Rev.* **38**, 2082–2083 (1931).
- ³⁵M. A. Anders, P. M. Lenahan, N. J. Harmon, and M. E. Flatté, “A technique to measure spin-dependent trapping events at the metal-oxide-semiconductor field-effect transistor interface: Near zero field spin-dependent charge pumping,” *J. Appl. Phys.* **128**, 244501 (2020).